

Efficient Trajectory Compression and Queries

Hongbo Yin , Hong Gao , Binghao Wang , Sirui Li , and Jianzhong Li

Department of Computer Science
Harbin Institute of Technology, Harbin, China
{hongboyin, honggao, wangbinghao, kuwylsr, lijzh}@hit.edu.cn

Abstract—Nowadays, there are ubiquitousness of GPS sensors in various devices collecting, storing and transmitting tremendous trajectory data. However, an unprecedented scale of GPS data has posed an urgent demand for not only an effective storage mechanism but also an efficient query mechanism. Line simplification in online mode, a kind of commonly used trajectory compression methods in practice, plays an important role to attack this issue. But for the existing algorithms, either their time cost is extremely high, or the accuracy loss after the compression is too much. To address this, we propose ϵ -Region based Online trajectory Compression with Error bounded (ROCE for short), which makes the best balance among the accuracy loss, the time cost and the compression rate. In most previous work, each trajectory is seen as a sequence of discrete points for various queries. But it's not suitable when the queried trajectories have been compressed, because there may be hundreds of points discarded between each two adjacent points and the points in each compressed trajectory are quite sparse. To attack this issue, in this paper, each compressed trajectory is regarded as a sequence of continuous line segments, but not discrete points. And based on this, we propose a new trajectory similarity metric AL, an efficient index *ASP-tree* and two algorithms about how to process range queries and top- k similarity queries on the compressed trajectories. Extensive experiments have been done on real datasets and the results demonstrate superior performance of our methods.

I. INTRODUCTION

The last decade has witnessed an unprecedented growth of mobile devices, such as smart-phones, vehicles, and wearable smart devices. Nearly all of them are equipped with the location-tracking function and widely used to collect massive trajectory data of moving objects at a certain sampling rate (e.g. 5 seconds) for location based services, trajectory mining, wildlife tracking and many other useful and meaningful applications. However, the amount of the trajectory data collected is often very large, and in many application scenarios, it's too difficult to store and query on such massive trajectories. For example, Fitbit, one of the most popular wearable device manufacturing companies for fitness monitors and activity trackers, has 28 million active users up to November 1st, 2019¹. If each wearable device records its latest position every 5 seconds, over 14 trillion trajectory points in total will be generated in just one month. It will consume too much network bandwidth to transmit such large amounts of data to the cloud server. And such large amounts of data also brings a great deal of hardship on storing and querying.

Trajectory compression is a suitable and effective solution to solve the problem. Line simplification, which compresses each trajectory into a set of continuous line segments, is a mainstream compression method and has drawn wide attention. It's a kind of lossy compression, where a high compression rate can be obtained with a tolerable error bound. Existing line simplification methods fall into two categories, i.e. batch mode and online mode. For each trajectory, algorithms in batch mode require that all points in this trajectory must be loaded in the local buffer before compression, which means that the local buffer must be large enough to hold the entire trajectory. Thus, the space complexities of these algorithms are at least $O(N)$, or even $O(N^2)$, which limits the application of these algorithms in resource-constrained environments. Therefore, more work focuses on the other kind of compression methods, algorithms in online mode, which only need a limited size of local buffer, rather than a very large local buffer, to compress trajectories in an online processing manner. Thus algorithms in online mode have much more application scenarios compared with those in batch mode, e.g. compressing streaming data. For all algorithms in online mode, the execution time, the accuracy loss and the compression rate are the three indicators used to measure their performance. There is a tradeoff among them, and the key issue is how to reach a good balance. For some algorithms, though their accuracy loss is small, their time cost is extremely high, such as BQS [1] and FBQS [1] in Table I, part of the experimental results of Zhang et al [2]. For other algorithms, the execution time needed by them is relatively less, but at the expense of the extremely high accuracy loss, such as Angular [3], Interval [4] and OPERB [5] in Table I. So, it's still a big challenge to compress trajectories into much smaller forms with less execution time and less accuracy loss. To address this, we propose a new online line simplification compression method, ϵ -Region based Online trajectory Compression with Error bounded (ROCE for short), with only $O(N)$ time complexity and $O(1)$ space complexity. When the compression rate is fixed, ROCE is one of the fastest algorithms, and its accuracy loss is the smallest among the fastest algorithms. ROCE makes the best balance among the accuracy loss, the time cost and the compression rate.

Compressing trajectories can help us reduce not only the cost of transmission and storage, but also the computing cost of queries. So how to process queries on compressed trajectories is very important. Range queries and top- k similarity queries are two kinds of most fundamental queries for various

¹<https://expandeddrablings.com/index.php/fitbit-statistics/>

TABLE I
THE TIME COST AND ACCURACY LOSS OF SOME COMPRESSION
ALGORITHMS IN ONLINE MODE

Compression Algorithm	BQS	FBQS	Angular	Interval	OPERB
Execution Time per Point (μs)	500.91	405.38	0.20	0.28	0.97
The Maximum PED Error	38.23	36.63	1532.65	1889.81	306.20

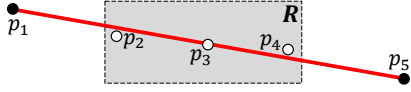


Fig. 1. An example that the discarded points p_2 , p_3 and p_4 are all in R , but neither endpoint of the line segment p_1p_5 falls in region R

applications in trajectory data analysis and they have attracted wide attention. In most previous work, each trajectory is seen as a sequence of discrete points. And it's usually regarded that a trajectory is overlapped with the query region R iff at least one point in this trajectory falls in R . However, this judgement condition is not complete in some situations where the points in each queried trajectory are very sparse. Especially for compressed trajectories, there may be hundreds of points discarded between each two adjacent points in compressed trajectories, which makes the points in compressed trajectories quite sparse. If some points in a trajectory fall in the the query region, but these points are discarded after the compression, such as the situation shown in Figure 1, then such a trajectory is missing in the result set. To address this, in this paper, each compressed trajectory is regarded as a sequence of continuous line segments, but not discrete points. And based on this, we propose two algorithms about how to process range queries and top- k similarity queries on the compressed trajectories.

The main contributions of this paper are summarized as follows:

- Point-to-Segment Euclidean Distance (PSED), a new accuracy loss metric, is defined to measure the degree of the accuracy loss after a trajectory is compressed. Then based on PSED, we propose a new online line simplification compression algorithm ROCE with bounded error. With only $O(N)$ time complexity and $O(1)$ space complexity, ROCE achieves the best balance among the accuracy loss, the time cost and the compression rate.
- To improve the accuracy of range query results on compressed trajectories, we propose a new range query processing algorithm RQC. F_1 , the synthesized indicator of the precision rate and the recall rate, can be improved greatly.
- A new trajectory similarity metric, Area clamped by the Line segments (AL for short), is defined to measure the similarity between each pair of compressed trajectories. And based on AL, we propose a new top- k similarity query processing algorithm SQC.
- An efficient index *ASP-tree* and a set of novel techniques are also presented to accelerate the processing of both range queries and top- k similarity queries greatly.
- We conduct extensive comparison experiments on real-life trajectory datasets, and the results demonstrate supe-

rior performance of our methods.

The rest of this paper is organized as follows. Section II introduces a new accuracy loss metric PSED and a new compression algorithm ROCE. Section III introduces an efficient index *ASP-tree* and the range query processing algorithm RQC. Section IV gives a new trajectory similarity metric AL and the top- k similarity query processing algorithm SQC. Section V shows the sufficient experimental results and analysis. Section VI reviews related works and finally Section VII concludes our work.

II. ROCE COMPRESSION ALGORITHM

In this section, we first propose an accuracy loss metric PSED. Then based on PSED, a new compression algorithm ROCE is introduced in detail.

A. Basic Concepts and Notations

A trajectory T can be expressed as a sequence of discrete points $\{p_1, p_2, \dots, p_N\}$, where $T[i] = p_i(x_i, y_i)$ represents the coordinate of the moving object. For any two points p_i and p_j , if $i < j$, then p_i was generated before p_j .

Given a trajectory $T = \{p_1, p_2, \dots, p_N\}$, $\forall i, j (1 \leq i < j \leq N)$, $T[i : j] = \{p_i, p_{i+1}, \dots, p_j\}$ represents a *trajectory segment* starting from p_i and ending at p_j with $(j - i + 1)$ points, and it can be approximately represented by the line segment $p_i p_j$, i.e., $p_i p_j$ is the compressed form of $T[i : j]$. $p_{i+1}, p_{i+2}, \dots, p_{j-1}$ are the discarded points, and $p_i p_j$ is called the corresponding line segments of p_i, p_{i+1}, \dots, p_j . Each trajectory can be divided into a set of consecutive trajectory segments.

Definition 1. (*Compressed Trajectory T'*): Given a trajectory $T = \{p_1, p_2, \dots, p_N\}$ consisting of a set of consecutive trajectory segments $\{T[i_1 : i_2], T[i_2 : i_3], \dots, T[i_{n-1} : i_n]\}$ ($i_1 = 1, i_n = N$), the corresponding compressed trajectory T' of T is a set of $n - 1$ consecutive line segments $p_{i_1} p_{i_2}, p_{i_2} p_{i_3}, \dots, p_{i_{n-1}} p_{i_n}$. To simplify the representation, T' can be denoted as $\{p_{i_1}, p_{i_2}, \dots, p_{i_n}\}$ ($p_{i_1} = p_1, p_{i_n} = p_N$).

In order to distinguish a trajectory from its corresponding compressed trajectory, we call it a raw trajectory in the following. Each raw trajectory is compressed into a set of consecutive line segments, and these consecutive line segments approximately describe the movement of the moving object.

Definition 2. (*Compression Rate*): Given a raw trajectory $T = \{p_1, p_2, \dots, p_N\}$ with N points and its compressed trajectory, $T' = \{p_{i_1}, p_{i_2}, \dots, p_{i_n}\}$ ($p_{i_1} = p_1, p_{i_n} = p_N$) with $n - 1$ consecutive line segments, the compression rate is

$$r = N/n.$$

B. Accuracy Loss Metric

After compression, a set of consecutive line segments is used to approximately represent a raw trajectory. When the compression rate is fixed, for a compression algorithm, the smaller accuracy loss, the better. How to measure the accuracy loss calls for a reasonable metric. Usually, the accuracy loss

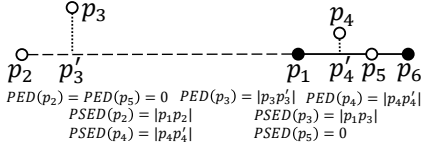


Fig. 2. An example shows how to calculate PED and PSED

is calculated based on the deviation between each discarded point and its corresponding line segment.

Perpendicular Euclidean Distance (PED for short), an accuracy loss metric adopted by most existing line simplification methods, e.g. [1], [5]–[7], is formally defined as:

Definition 3. (PED): Given a trajectory segment $T[s : e](s < e)$ and its compressed form, the line segment $p_s p_e$, for any discarded point $p_m(s < m < e)$ in $T[s : e]$, the PED of p_m is calculated as:

$$PED(p_m) = \frac{\|\overrightarrow{p_s p_m} \times \overrightarrow{p_s p_e}\|}{\|\overrightarrow{p_s p_e}\|}$$

where \times is the symbol of cross product in vector operations and $\|\cdot\|$ is to calculate the length of a vector.

PED measures the deviation by using the shortest Euclidean distance from each discarded point to the straight line where the corresponding line segment of this discarded point lies. PED is suitable to the situations where the moving direction doesn't change sharply. However, when the change of the moving direction in angle is more than 90 degrees, e.g., a car makes a sharp turn, PED can hardly describe the deviation accurately. Figure 2 illustrates an example that the moving object makes an u-turn and the trajectory segment $T[1 : 6]$ is approximately represented by the line segment $p_1 p_6$. The accuracy loss of p_2 in PED is 0 and the accuracy loss of p_3 in PED is $|p_3 p'_3|$. But in fact, p_2 is obviously far away from $p_1 p_6$ and the distance between p_3 and the line segment $p_1 p_6$ is far more than $|p_3 p'_3|$. The reason is that $PED(p_2)$ and $PED(p_3)$ are both calculated based on the perpendicular distance between the discarded points and the extension line of $p_1 p_6$. Thus the compressed trajectories, which are generated by the compression algorithms based on PED, are not able to reflect the real movement patterns.

To solve this problem, we define a new accuracy loss metric, Point-to-Segment Euclidean Distance (PSED for short), which is a revised version of PED, to measure the accuracy loss. The main difference between PSED and PED is that PSED adopts the shortest Euclidean distance from a point to its corresponding line segment, rather than the straight line where the corresponding line segment lies. PSED is formally defined as follows:

Definition 4. (PSED): Given a trajectory segment $T[s : e](s < e)$ and its compressed form, the line segment $p_s p_e$, for any discarded point $p_m(s < m < e)$ in $T[s : e]$, the PSED of p_m is calculated according to the following cases:

$$PSED(p_m) = \begin{cases} \frac{\|\overrightarrow{p_s p_m} \times \overrightarrow{p_s p_e}\|}{\|\overrightarrow{p_s p_e}\|} & \overrightarrow{p_s p_m} \cdot \overrightarrow{p_s p_e} \geq 0 \text{ and } \overrightarrow{p_m p_e} \cdot \overrightarrow{p_s p_e} \geq 0 \\ \min\{\|\overrightarrow{p_s p_m}\|, \|\overrightarrow{p_m p_e}\|\} & \text{otherwise} \end{cases}$$

where \times and \cdot are respectively the symbols of cross product and dot product in vector operations.

In Definition 4, if $\overrightarrow{p_s p_m} \cdot \overrightarrow{p_s p_e} \geq 0$ and $\overrightarrow{p_m p_e} \cdot \overrightarrow{p_s p_e} \geq 0$, i.e., the perpendicular point of p_m falls on the line segment $p_s p_e$, $PSED(p_m)$ is the perpendicular distance from p_m to $p_s p_e$, the same as $PED(p_m)$. Otherwise, $PSED(p_m)$ is the smaller one of $|p_s p_m|$ and $|p_m p_e|$.

In Figure 2, since the perpendicular points of p_2 and p_3 both fall on the extension line of $p_1 p_6$, $PSED(p_2) = |p_1 p_2|$ and $PSED(p_3) = |p_1 p_3|$. For the perpendicular points of p_4 and p_5 are both on the line segment $p_1 p_6$, $PSED(p_4) = PED(p_4) = |p_4 p'_4|$ and $PSED(p_5) = PED(p_5) = 0$.

With the definition of PSED, the ϵ -error-bounded compressed trajectory is defined as follows:

Definition 5. (ϵ -error-bounded Compressed Trajectory): Given a value ϵ , a raw trajectory $T = \{p_1, p_2, \dots, p_N\}$ and its compressed trajectory $T' = \{p_{i_1}, p_{i_2}, \dots, p_{i_n}\}$ ($p_{i_1} = p_1, p_{i_n} = p_N$), for each discarded point p_m in T , the accuracy loss metric $PSED(p_m) \leq \epsilon$. Then we say T' is ϵ -error-bounded and ϵ is the upper bound of PSED.

C. Algorithm ROCE

In this part, we present a new trajectory compression algorithm ROCE, which makes the best balance among the accuracy loss, the time cost and the compression rate. Given a raw trajectory $T = \{p_1, p_2, \dots, p_N\}$ and the upper bound of PSED ϵ , ROCE is to compress T into an ϵ -error-bounded compressed trajectory T' , which is a set of consecutive line segments.

In order to determine whether a compressed trajectory is ϵ -error-bounded more conveniently, we define a new concept ϵ -Region as below:

Definition 6. (ϵ -Region): Given a raw trajectory point p_i and the upper bound of PSED ϵ , the circle region, whose center is p_i and radius is ϵ , is called the ϵ -Region of p_i .

For convenience, E_i is used to denote the ϵ -Region of p_i in the following. We can easily get the property as below:

Lemma 1. Given a trajectory segment $T[s : e](s < e)$ and the upper bound of PSED ϵ , $T[s : e]$ is compressed into a line segment $p_s p_e$. For any discarded point $p_m(s < m < e)$ in $T[s : e]$, $PSED(p_m) \leq \epsilon$ iff $p_s p_e$ intersects E_i . Then, $p_s p_e$ is ϵ -error-bounded iff $p_s p_e$ intersects all ϵ -Regions of discarded points, i.e. $E_{s+1}, E_{s+2}, \dots, E_{e-1}$.

In Figure 3, the trajectory segment $T[1 : 3]$ is compressed into the line segment $p_1 p_3$. It's obvious that the line segment $p_1 p_3$ doesn't intersect E_2 and $PSED(p_2) > \epsilon$. Thus $p_1 p_3$ isn't ϵ -error-bounded. Another trajectory segment $T[11 : 16]$ is compressed into the line segment $p_{11} p_{16}$. For any discarded point, $p_{11} p_{16}$ intersects its corresponding ϵ -Region, and $p_{11} p_{16}$ is ϵ -error-bounded.

Given a raw trajectory $T = \{p_1, p_2, \dots, p_N\}$ and the upper bound of PSED ϵ , an optimal compression is to compress T into an ϵ -error-bounded trajectory T' , which consists of the

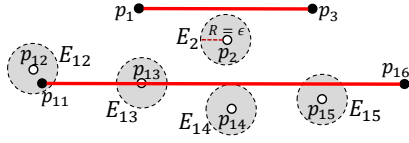


Fig. 3. $T[1 : 3]$ and $T[11 : 16]$ are two trajectory segments and are compressed into the line segments p_1p_3 and $p_{11}p_{16}$ respectively

smallest number of consecutive line segments. T can be split into 2^{N-1} different sets of consecutive trajectory segments, which means there are up to 2^{N-1} different compressed strategies. So, the search space is exponential. By adopting a greedy strategy and some effective tricks, ROCE handles the trajectory compression in an online processing manner. First, ROCE anchors the start point p_s of a trajectory segment to be compressed. p_f , where f is a variable and assigned as $(s + 2)$ at first, is selected as the current float point. Then a trajectory segment $T[s : f]$ is defined by using p_s and p_f . If $\forall p_m (s < m < f) \in T[s : f]$, $PSED(p_m) \leq \epsilon$, then p_{f+1} is assigned as the new float point and $f + 1$ is assigned as f . Otherwise, p_{f-1} becomes the end point of the current trajectory segment, and the current trajectory segment $T[s : f - 1]$ is compressed into a line segment $p_s p_{f-1}$. And p_{f-1} becomes the anchor point of the next trajectory segment to be compressed.

Every time ROCE checks whether the last float point p_{f-1} is final end point of the current trajectory segment, each point $p_m (s < m < f)$ needs to be scanned once to calculate PSED to verify whether $p_s p_f$ is ϵ -error-bounded. So each point needs to be scanned multiple times during the compression. To deal with this problem, the candidate region is adopted by ROCE, and each point needs to be scanned once and only once. (p_s, p_f) -CandidateRegion and $T[s : f]$ -CandidateRegion are formally defined as follows:

Definition 7. ((p_s, p_f) -CandidateRegion): Given the upper bound of PSED ϵ , a trajectory segment $T[s : f] (s < f$ and $|p_s p_f| > \epsilon)$. Since p_s is outside the corresponding ϵ -Region E_f of p_f , we can get two tangent rays of E_f starting from p_s named $tr_{s,f}$ and $tr'_{s,f}$. The minor sector enclosed by $tr_{s,f}$ and $tr'_{s,f}$, minus the overlapping region of this minor sector and a circular region, whose center and radius are p_s and $|p_s p_f|$ respectively, is (p_s, p_f) -CandidateRegion.

Definition 8. ($T[s : f]$ -CandidateRegion): Given the upper bound of PSED ϵ , a trajectory segment $T[s : f] (s < f$ and $|p_s p_f| > \epsilon)$. $T[s : f]$ -CandidateRegion = (p_s, p_{s+1}) -CandidateRegion \cap (p_s, p_{s+2}) -CandidateRegion \cap ... \cap (p_s, p_f) -CandidateRegion, i.e., if $s < (f - 1)$, $T[s : f]$ -CandidateRegion = $T[s : f - 1]$ -CandidateRegion \cap (p_s, p_f) -CandidateRegion.

During the procedure of finding which point is the final end point of the current trajectory segment starting from p_s , if the float point p_{f+1} falls in $T[s : f]$ -CandidateRegion, then for any point $p_m (s < m < f + 1)$, $PSED(p_m)$ must be no more than ϵ . So by using the candidate region, PSED no longer

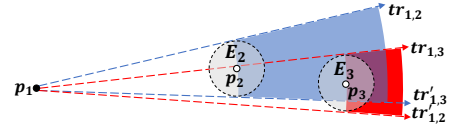


Fig. 4. An example of ROCE

needs to be calculated, and each point needs to be scanned once and only once.

Figure 4 gives us an example to show the processing procedure of ROCE. Since p_1 is outside the corresponding ϵ -Region E_2 of p_2 , we can get two tangent rays $tr_{1,2}$ and $tr'_{1,2}$ of E_2 . The region in blue is both (p_1, p_2) -CandidateRegion and $T[1 : 2]$ -CandidateRegion. p_3 falls in $T[1 : 2]$ -CandidateRegion. Similarly, we can get (p_1, p_3) -CandidateRegion, which is the region in red. The overlapping region of $T[1 : 2]$ -CandidateRegion and (p_1, p_3) -CandidateRegion is $T[1 : 3]$ -CandidateRegion. If the next point p_4 falls in $T[1 : 3]$ -CandidateRegion, the line segment $p_1 p_4$ must intersect all ϵ -Regions of discarded points, i.e., E_2 , E_3 , and $p_1 p_4$ must be ϵ -error-bounded according to Lemma 1. Otherwise, the trajectory segment $T[1 : 3]$ is compressed into $p_1 p_3$. And ROCE will repeat the similar processing procedure starting from p_3 until the last point is compressed.

ROCE is formally described in Algorithm 1. Starting from the first point, ROCE scans points in the trajectory one by one. In each iteration, ROCE tries to find which point is the final end point of the current trajectory segment, and this trajectory segment is compressed into a line segment (Line 4-15). For the following points of the start point, if their ϵ -Regions all contain the start point, any line segment starting from the start point must intersect their corresponding ϵ -Regions. Thus their restrictions no longer need to be thought about according to Lemma 1 (Line 7-9).

By using the candidate region, each point needs to be scanned once and only once. So ROCE is a one-pass error bounded trajectory compression algorithm, and its time complexity is $O(N)$. Only const space is needed by ROCE, no matter how many points to be compressed into a line segment. Thus, the space complexity of ROCE is only $O(1)$.

III. RANGE QUERY PROCESSING

In most previous work, a trajectory is thought to be overlapped with the query region R iff at least one point in this trajectory falls in R . However, this judgement condition is not complete especially for compressed trajectories, because there may be hundreds of points discarded between each two adjacent points, and the points in each queried trajectory are extremely sparse. If some points in a raw trajectory fall in the the query region, but these points are discarded after the compression, then such a trajectory is missing in the result set. To address this, each compressed trajectory is regarded as a set of continuous line segments, but not discrete points. And based on this, we propose a new Range Query processing algorithm on Compressed trajectories (RQC for short). A range query is redefined as:

Algorithm 1 The ROCE Algorithm

Input: Raw trajectory $T = \{p_1, p_2, \dots, p_N\}$, the upper bound of PSED ϵ

Output: ϵ -error-bounded compressed trajectory $T' = \{p_{i_1}, p_{i_2}, \dots, p_{i_n}\} (p_{i_1} = p_1, p_{i_n} = p_N)$ of T

```

1:  $i = 1$ 
2:  $T' = [T[1]]$ 
3: while  $i \leq N$  do
4:    $StartPoint = T[i]$ 
5:    $Initialize(CandidateRegion, StartPoint)$ 
6:    $i = i + 1$ 
7:   while ( $StartPoint$  in  $EpsilonRegion(T[i], \epsilon)$ ) and ( $i \leq N$ ) do
8:      $i = i + 1$ 
9:   end while
10:  while ( $T[i]$  in  $CandidateRegion$ ) and ( $i \leq N$ ) do
11:     $UpdateCandidateRegion(CandidateRegion, T[i], \epsilon)$ 
12:     $i = i + 1$ 
13:  end while
14:   $i = i - 1$ 
15:   $T'.Append(T[i])$ 
16: end while
17: return  $T'$ 

```

Definition 9. (Range Query): Given a compressed trajectory dataset \mathbb{T} and a query region R , the range query result $Q_r(R, \mathbb{T})$ consists of all such compressed trajectories in \mathbb{T} , at least one of whose line segments intersects R , i.e.,

$$Q_r(R, \mathbb{T}) = \{T \in \mathbb{T} | \exists p_{i_k}, p_{i_{k+1}} \in T, \text{ s.t. } p_{i_k}, p_{i_{k+1}} \text{ intersects } R\}$$

For simplicity, we consider query regions as two-dimensional rectangles, but our approach can be adapted to handle regions in arbitrary shapes.

In order to get the query result $Q_r(R, \mathbb{T})$ of a given range query, a key issue is to determine whether a line segment intersects the query region R . There are lots of work on how to determine the relationship between a line segment and a rectangle, so we don't discuss about that in this paper. However, each compressed trajectory consists of multiple consecutive line segments, and it costs a lot to judge the relationship between the query region R and each line segments in all compressed trajectories. To attack this issue, in Section III-A, some accelerating strategies are proposed to reduce the size of the search space. We also propose a highly efficient index to further speed up range queries in Section III-B.

A. Accelerating Strategies

In order to reduce the size of the search space and accelerate range queries, the Minimal Bounding Rectangle (MBR for short) of a compressed trajectory is used here. $MBR(T')$ is the smallest rectangle which contains the entire compressed trajectory T' . We can easily get an observation as below:



Fig. 5. The rectangle in gray represents the query region R and the rectangle in orange represents $MBR(T')$

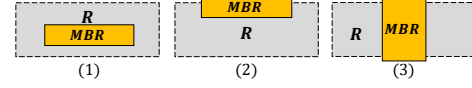


Fig. 6. Each gray rectangle represents the query region R and each orange rectangle represents $MBR(T')$

Observation 1. Given a query region R , a compressed trajectory T' and its MBR $MBR(T')$, if $MBR(T')$ and R don't overlap, T' must not be overlapped with R .

If $MBR(T')$ and R overlap, it's not sure whether T' is overlapped with R , such as the situation shown in Figure 5. Under this circumstance, we have another observation. As shown in Figure 6, there are still 3 cases where T' must be overlapped with R .

Observation 2. Given a query region R , and a compressed trajectory T' .

(1) T' must be overlapped with R if $MBR(T')$ is contained in R .

(2) If there is an edge of $MBR(T')$ completely contained in R , then at least one point of T' is in R , and T' must be overlapped with R . The reason is that based on the concept of MBR, there must be at least one point of T' on each edge of $MBR(T')$.

(3) There are only two parallel edges of $MBR(T')$ intersecting R , and the other two parallel edges outside R . From the analysis in Case (2), we can get that there is at least one point of T' on each parallel edge which is outside R . For T' consists of multiple continuous line segments, these two points must be connected by continuous line segments. So, there must be at least one line segment in T' intersecting R and T' must be overlapped with R .

B. Trajectory Index ASP-tree

In order to further speed up range queries, we propose a highly efficient index, Adaptive Spatial Partition quadtree like index (*ASP-tree* for short). In order to reduce the space overhead, only leaf nodes directly store trajectory information in *ASP-tree*. For each non-leaf node in *ASP-tree*, it contains entries in the form of (*ChildRegion-ChildPointer*), where *ChildRegion-ChildPointer* refers to the corresponding regions and addresses of its 4 child nodes. Each leaf node in *ASP-tree* stores information in the form of (*ID-LineSegments*). (*ID-LineSegments*) refers to continue line segments of a compressed trajectory whose identifier is *ID*, and these line segments all intersect the corresponding region of this leaf node.

There is only a root node, which represents the whole region and all compressed trajectories. For each node in *ASP-tree*,

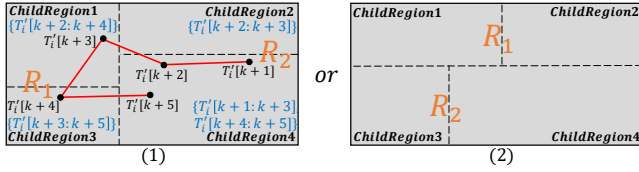


Fig. 7. An example shows how to divide the corresponding region of a father node and how to split the line segments intersecting the corresponding region of the father node among its 4 child nodes

if there are more than ξ line segments which intersect the corresponding region of this node, then this node is a non-leaf node which has 4 child nodes. Otherwise, this node is a leaf node. So ξ , a threshold value estimated through experiments, controls the height of *ASP-tree*.

Given how to divide the corresponding region of a non-leaf node, the line segments intersecting the corresponding region should be split among the 4 child nodes of this node. The strategy is to verify which one or more corresponding regions of these 4 child nodes each line segment intersects, and then assign this line segment to the corresponding child nodes. So a line segment may be stored in different leaf nodes. As an example shown in Figure 7, there are 4 continue line segments in T'_i intersecting the father node. The line segment $T'_i[k+2]T'_i[k+3]$ intersects *ChildRegion1*, *ChildRegion2* and *ChildRegion4*, so $T'_i[k+2]T'_i[k+3]$ is assigned to these 3 corresponding child nodes. And finally, 3 line segments $T'_i[k+1]T'_i[k+2]$, $T'_i[k+2]T'_i[k+3]$ and $T'_i[k+4]T'_i[k+5]$ are assigned to the child node whose corresponding region is *ChildRegion4*.

In a traditional quadtree, if a node has 4 child nodes, the corresponding region of the father node is evenly divided into four regions. But it's not suitable to do so, because trajectories are usually not uniformly distributed. This may make the index inclined greatly, which affects the efficiency of range queries. To handle this, a data adaptive strategy is adopted in *ASP-tree*. There are totally two cases to divide the corresponding region of a father node among its 4 child nodes as shown in Figure 7. For all line segments intersecting the corresponding region of the father node, we first get all endpoints of these line segments falling in the this region, and then calculate the median of all their x dimensions (y dimensions). The result of this calculation is used to draw a vertical (horizontal) line, which divides the region represented by the father node into two smaller regions, R_1 and R_2 . After that, for all endpoints of the line segments falling in R_1 and R_2 , the median of all y dimensions (x dimensions) of all these endpoints are respectively used to further divide these two parts into 4 regions. For these two case, the case with fewer repeated line segments assigned to the 4 child nodes will be chosen. The purpose for doing these is to make *ASP-tree* as balanced as possible. There may be a special case when a region is to be divided into 2 parts. For all line segment intersecting this region, none of their endpoints fall in this region. In such a case, we divide this region evenly into 2 equal regions.

Let's introduce how to get the range query result $Q_r(R, \mathbb{T})$

on compressed trajectories with *ASP-tree*. First, traverse *ASP-tree* from top to bottom with the query region R to find all leaf nodes whose corresponding regions are overlapped with R , and then put all continue line segments stored in these leaf nodes into the candidate result set. For a non-leaf node, if its corresponding region isn't overlapped with R , then the corresponding regions of its descendants must be not overlapped with R and its descendants no longer need to be traversed. If the corresponding region of a leaf node is completely contained in R , then directly put the identifiers of all continue line segments stored in this node into the final result set. Second, for continue line segments in the candidate result set, we use their MBRs to determine their relationships with R one by one. Third, if the relationship still can't be judged, then we go to check whether there is a line segment in these continue line segments intersecting R . After these three steps, we can get the range query result $Q_r(R, \mathbb{T})$.

IV. SIMILARITY QUERY PROCESSING

In this section, a new trajectory similarity metric, Area clamped by the Line segments (AL for short), is introduced first. Then based on AL, we propose a top- k Similarity Query processing algorithm on Compressed trajectories (SQC for short).

A. Trajectory Similarity Metric AL

The trajectory similarity measure is a fundamental operation that can be used in many applications, e.g. similarity search, clustering and classification. Given two compressed trajectories $T'_r = \{p_{i_1}, p_{i_2}, \dots, p_{i_m}\}$ and $T'_s = \{p_{j_1}, p_{j_2}, \dots, p_{j_n}\}$. Most widely used trajectory similarity metrics are based on the distance between matched point pairs of T'_r and T'_s . This is suitable for raw trajectories where the distance between any two adjacent points in a trajectory doesn't vary much. But for compressed trajectories, a few or even hundreds of raw points are approximately represented by a line segment, which makes the length of each line segment vary greatly. So these similarity metrics are unapplicable. As shown in Figure 8, there are two pairs of matched line segments in compressed trajectories T'_r and T'_s . There is no doubt that the pair with longer lengths, i.e. $p_{i_1}p_{i_2}$ and $p_{j_1}p_{j_2}$, should have a greater impact on the degree of similarity between T'_r and T'_s than $p_{i_2}p_{i_3}$ and $p_{j_2}p_{j_3}$. Thus, the lengths of line segments should also be considered when we define the similarity between two compressed trajectories.

When we measure the similarity between T'_r and T'_s with different numbers of line segments, there must be unmatched line segments in the compressed trajectory with more line segments, e.g. $p_{i_3}p_{i_4}$ in T'_r as shown in Figure 8. The existence of the line segment $p_{i_3}p_{i_4}$ has a negative effect on the similarity between T'_r and T'_s , since there is no line segment in T'_s matched with $p_{i_3}p_{i_4}$. So such a line segment should be punished when we measure the similarity between T'_r and T'_s .

For a pair of line segments $p_{i_k}p_{i_{k+1}}$ and $p_{j_h}p_{j_{h+1}}$, each line segment is divided into at most two parts, the matched part and the unmatched part. The matched part of a line segment is a subline segment satisfying the condition that for

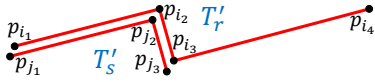


Fig. 8. T'_r and T'_s consist of 3 and 2 consecutive line segments respectively

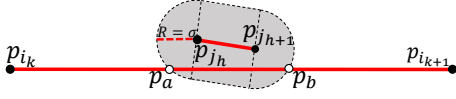


Fig. 9. Based on $p_{j_h}p_{j_{h+1}}$, the line segment $p_{i_k}p_{i_{k+1}}$ is divided into 2 parts

any point on this subline segment, its minimum Euclidean distance to the other line segment is no more than σ , a given threshold value. As shown in Figure 9, the matched part of $p_{i_k}p_{i_{k+1}}$ is the subline segment $p_a p_b$, and the unmatched part of $p_{i_k}p_{i_{k+1}}$ is the remaining two subline segments, i.e. $p_{i_k}p_a$ and $p_b p_{i_{k+1}}$. Let $Dist(p_{i_k}p_{i_{k+1}}, p_{j_h}p_{j_{h+1}})$ denote the dissimilarity between $p_{i_k}p_{i_{k+1}}$ and $p_{j_h}p_{j_{h+1}}$, and then $Dist(p_{i_k}p_{i_{k+1}}, p_{j_h}p_{j_{h+1}}) = C(p_{i_k}p_{i_{k+1}}, p_{j_h}p_{j_{h+1}}) + P(p_{i_k}p_{i_{k+1}}, p_{j_h}p_{j_{h+1}})$, where $C(p_{i_k}p_{i_{k+1}}, p_{j_h}p_{j_{h+1}})$ is the area clamped by two matched parts, and $P(p_{i_k}p_{i_{k+1}}, p_{j_h}p_{j_{h+1}})$ is the total penalty areas of two unmatched parts. $P(p_{i_k}p_{i_{k+1}}, p_{j_h}p_{j_{h+1}}) = \sum_{p_{u_1}p_{u_2} \in 2UP} Punish(p_{u_1}p_{u_2})$ and $Punish(p_{u_1}p_{u_2}) = |p_{u_1}p_{u_2}| * (\sigma/2)$, where $2UP$ denotes two unmatched parts of $p_{i_k}p_{i_{k+1}}$ and $p_{j_h}p_{j_{h+1}}$, $p_{u_1}p_{u_2}$ is an unmatched line segment or subline segment in $2UP$, and $|p_{u_1}p_{u_2}|$ is to calculate the length of $p_{u_1}p_{u_2}$. Next, let's introduce how to calculate $C(p_{i_k}p_{i_{k+1}}, p_{j_h}p_{j_{h+1}})$. S_{abc} represents the area of the triangle whose 3 vertices are p_a , p_b and p_c . Assuming the subline segments $p_a p_b$ and $p_c p_d$ are the matched parts of $p_{i_k}p_{i_{k+1}}$ and $p_{j_h}p_{j_{h+1}}$ respectively, $C(p_{i_k}p_{i_{k+1}}, p_{j_h}p_{j_{h+1}})$, the area clamped by $p_a p_b$ and $p_c p_d$, is calculated in four situations as shown in Figure 10:

- (1) If $p_a p_b p_c p_d$ is a convex quadrilateral, then $C(p_{i_k}p_{i_{k+1}}, p_{j_h}p_{j_{h+1}}) = S_{abd} + S_{bcd}$.
- (2) If two points p_a and p_b are on the different regions divided by the straight line where $p_c p_d$ lies, then $C(p_{i_k}p_{i_{k+1}}, p_{j_h}p_{j_{h+1}}) = S_{acd} + S_{bcd}$.
- (3) If one point p_c is on the straight line where $p_a p_b$ lies, then $C(p_{i_k}p_{i_{k+1}}, p_{j_h}p_{j_{h+1}}) = S_{abd}$.
- (4) If $p_a p_b$ and $p_c p_d$ are collinear, then $C(p_{i_k}p_{i_{k+1}}, p_{j_h}p_{j_{h+1}}) = 0$.

Given two compressed trajectories $T'_r = \{p_{i_1}, p_{i_2}, \dots, p_{i_m}\}$ and $T'_s = \{p_{j_1}, p_{j_2}, \dots, p_{j_n}\}$, let $\Theta(T'_r, T'_s)$ represent the dissimilarity between T'_r and T'_s , and then $\Theta(T'_r, T'_s)$ can be

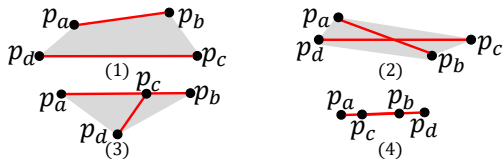


Fig. 10. The gray region is the region clamped by $p_a p_b$ and $p_c p_d$

recursively calculated as: $\Theta(T'_r, T'_s) =$

$$\begin{cases} Punish(T'_r) & \text{if } n = 1 \\ Punish(T'_s) & \text{if } m = 1 \\ \min \left\{ \begin{array}{l} Punish(p_{i_1}p_{i_2}) + \Theta(Rest(T'_r), T'_s), \\ Punish(p_{j_1}p_{j_2}) + \Theta(T'_r, Rest(T'_s)), \\ Dist(r'_1, s'_1) + \Theta(Rest(T'_r), Rest(T'_s)) \end{array} \right\} & \text{otherwise} \end{cases}$$

where $Punish(T'_r) = \sum_{k=1}^{m-1} Punish(p_{i_k}p_{i_{k+1}})$, $Punish(T'_s) = \sum_{h=1}^{n-1} Punish(p_{j_h}p_{j_{h+1}})$, $Rest(T'_r) = \{p_{i_2}, p_{i_3}, \dots, p_{i_m}\}$ and $Rest(T'_s) = \{p_{j_2}, p_{j_3}, \dots, p_{j_n}\}$.

$\Theta(T'_r, T'_s) = 0$ iff T'_r and T'_s are identical. If $\forall p_{i_k}p_{i_{k+1}} \in T'_r$ and $\forall p_{j_h}p_{j_{h+1}} \in T'_s$, there is no matched subline segment in $p_{i_k}p_{i_{k+1}}$ and $p_{j_h}p_{j_{h+1}}$, i.e., T'_r and T'_s are too far away from each other, then $\Theta(T'_r, T'_s) = Punish(T'_r) + Punish(T'_s)$. In general, $0 \leq \Theta(T'_r, T'_s) \leq Punish(T'_r) + Punish(T'_s)$. The similarity between T'_r and T'_s is represented by $AL(T'_r, T'_s)$, and then by normalizing $\Theta(T'_r, T'_s)$ into $[0, 1]$, $AL(T'_r, T'_s)$ is formally defined as:

Definition 10. (AL): Given two compressed trajectories T'_r and T'_s ,

$$AL(T'_r, T'_s) = 1 - \frac{\Theta(T'_r, T'_s)}{Punish(T'_r) + Punish(T'_s)}$$

The more similar T'_r and T'_s , the larger $AL(T'_r, T'_s)$.

B. AL Based Top-k Similarity Query

Definition 11. (Top-k Similarity Query): Given a query compressed trajectory T'_q , a compressed trajectory dataset \mathbb{T} , a distance threshold σ and an integer k , the top-k similarity query result $Q_s(T'_q, k, \mathbb{T}, \sigma)$ consists of k trajectories in \mathbb{T} , which are most similar to T'_q , satisfying: $\forall T'_1 \in Q_s(T'_q, k, \mathbb{T}, \sigma)$ and $\forall T'_2 \in (\mathbb{T} - Q_s(T'_q, k, \mathbb{T}, \sigma))$, $AL(T'_1, T'_q) \geq AL(T'_2, T'_q)$.

Like most widely used trajectory similarity measures, the computing of AL needs quadratic computation cost. So performing sequential scans across the entire dataset is not scalable. In addition, AL is also non-metric due to violating triangular inequality.

Theorem 1. AL doesn't satisfy triangular inequality.

Proof. Given three compressed trajectories, $T'_1 = \{(0, 0), (4, 0)\}$, $T'_2 = \{(0, 0), (4, 0), (4, 1), (7, 1)\}$ and $T'_3 = \{(0, 0), (4, 0), (4, -1), (5, -1)\}$, and σ , which is set to 5. Then, $AL(T'_1, T'_2) = \frac{1}{3}$, $AL(T'_1, T'_3) = \frac{1}{5}$, $AL(T'_2, T'_3) = \frac{4}{35}$ and $AL(T'_1, T'_3) + AL(T'_2, T'_3) < AL(T'_1, T'_2)$. Therefore, AL doesn't satisfy triangular inequality. \square

Because of Theorem 1, generic indexing techniques, which rely on triangular inequality based pruning, can't be applied here. In order to reduce the search space, we construct a candidate set to avoid lots of unnecessary calculations of AL. Before introducing the candidate set, we define a new concept, the σ -Bounding Rectangle (σ -BR for short) of a compressed trajectory.

Definition 12. (σ -BR(T')): Given a distance threshold σ and the MBR of a compressed trajectory T' , whose coordinate is

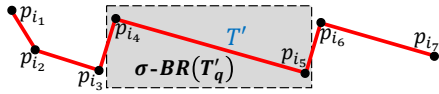


Fig. 11. An example shows how to accelerate the calculation of AL

represented by $[x'_{min}, x'_{max}] * [y'_{min}, y'_{max}]$, $\sigma\text{-BR}(T'_q)$ is a rectangle region, whose coordinate is $[x'_{min} - \sigma, x'_{max} + \sigma] * [y'_{min} - \sigma, y'_{max} + \sigma]$.

Based on Definition 12, the similarity candidate set is formally defined as:

Definition 13. (Similarity Candidate Set $\mathbb{SC}(T'_q, \mathbb{T}, \sigma)$): Given a query compressed trajectory T'_q , a compressed trajectory dataset \mathbb{T} and a distance threshold σ , the similarity candidate set $\mathbb{SC}(T'_q, \mathbb{T}, \sigma)$ consists of all compressed trajectories in \mathbb{T} , which are overlapped with $\sigma\text{-BR}(T'_q)$.

By using our range query processing algorithm RQC, we can get the similarity candidate set $\mathbb{SC}(T'_q, \mathbb{T}, \sigma)$. For any trajectory $T' \in (\mathbb{T} - \mathbb{SC}(T'_q, \mathbb{T}, \sigma))$, the similarity between T' and T'_q must be 0 in AL. To get the final result set $Q_s(T'_q, k, \mathbb{T}, \sigma)$, the AL between T'_q and each compressed trajectory in $\mathbb{SC}(T'_q, \mathbb{T}, \sigma)$ needs to be checked one by one. During this procedure, a smallest heap, whose size is k , is maintained and updated continuously.

By using the similarity candidate set, the searching space is reduced greatly, but the calculation cost of the AL between T'_q and each compressed trajectory in $\mathbb{SC}(T'_q, \mathbb{T}, \sigma)$ is still a little high. To address this, we propose an efficient *Pre-Punishment* strategy to reduce the cost. For a compressed trajectory T' in $\mathbb{SC}(T'_q, \mathbb{T}, \sigma)$, there may be some line segments in T' not intersecting $\sigma\text{-BR}(T'_q)$, such as the line segments $p_{i_1}p_{i_2}$, $p_{i_2}p_{i_3}$ and $p_{i_6}p_{i_7}$ in Figure 11. According to the definition of $\sigma\text{-BR}(T'_q)$, the distances of these line segments to any line segment in T'_q must be larger than σ , thus these line segments must be punished in the calculation of AL. So for each of these line segments, only *Punish()* of it needs to be calculated and the calculation of *Dist()* between it and each line segment in T'_q is not needed any more. In the same way, there may be also some line segments in T'_q not intersecting $\sigma\text{-BR}(T')$ and these line segments are sure to be punished in the calculation of AL. And for each of these line segments, only its corresponding *Punish()* needs to be calculated and the calculation of *Dist()* between it and each line segment in T' is also no longer needed. The experiment in section V-D3 shows that by using the *Pre-Punishment* strategy, the execution time of similarity queries can be reduced to as low as 17.8%.

V. EXPERIMENTAL EVALUATION

In this section, we evaluate the performance of our compression algorithm ROCE, and two query processing algorithms RQC and SQC.

A. Experiment Setup

1) *Datasets*: The experiments were conducted on 3 real-life datasets. The dataset Animal² [8] records the migration of 8 young white storks originating from 8 populations, and the sampling rates of these trajectories are relatively low. The dataset Indoor³ [9] records the trajectories of visitors in a shopping center, and the points in these trajectories were sampled quite frequently. With a very large size, the dataset Planet⁴ consists of quite a few trajectories distributed all over the globe, and the movement modes of these trajectories are very rich. These trajectories are sparsely distributed on the Earth, but mainly distributed in a large rectangular region, which is $3.9 * 10^5 km^2$ in area. All trajectories completely contained in this large region were selected as the raw dataset called Planet I. Since this dataset was to be compressed, the trajectories with less than 1000 points were removed. With 0.3 billion points in total, Planet I consists of 96279 raw trajectories.

When comparing the execution time of different compression algorithms, we found some baseline algorithms were too time-consuming to run on the entire datasets. So we randomly sampled some long trajectories from Animal, Indoor and Planet I. Then we got 3 subsets with 120, 90 and 47 long trajectories, and these subsets are called Animal II, Indoor II and Planet II respectively. There are all about 2 million points in these three subsets.

2) *Experimental Environment*: Experiments were all conducted on a linux machine with a 64-bit, 8-core, 3.6GHz Intel(R) Core (TM) i9-9900K CPU and 32GB memory. Our algorithms were all implemented in C++ on Ubuntu 18.04. Each experiment was repeated over 3 times and the average was reported here.

B. Performance Evaluation for Trajectory Compression Algorithms

We compared our compression algorithm ROCE with 4 existing trajectory compression algorithms in online mode, which use PED as their error metric, i.e. OPW(BOPW) [6], [7], BQS [1], FBQS [1] and OPERB [5]. Though the error metric of DOTS [10] is not PED but LISSSED, it was still compared with ROCE, because it was demonstrated stable superiority against other online compression algorithms on some indicators [2]. For these compression algorithms, their performances were measured by the execution time and accuracy loss.

1) *Execution Time*: In the first experiment, we evaluate the execution time of 6 algorithms w.r.t. varying the compression rate, and the results are shown in Figure 12. The results show that ROCE, OPW and OPERB are obviously faster than BQS, FBQS and DOTS. At the beginning of each loop iteration to compress a trajectory segment into a line segment, BQS and FBQS are more time-consuming than other algorithms. DOTS needs much more memory and time to handle the situations

²<http://dx.doi.org/10.5441/001/1.78152p3q>

³https://irc.atr.jp/crest2010_HRI/ATC_dataset/

⁴<https://wiki.openstreetmap.org/wiki/Planet.gpx>

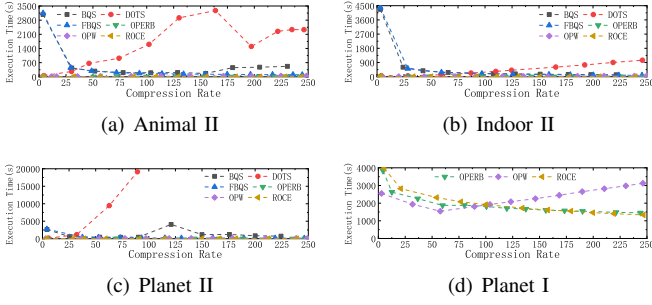


Fig. 12. Efficiency evaluation: varying the compression rate

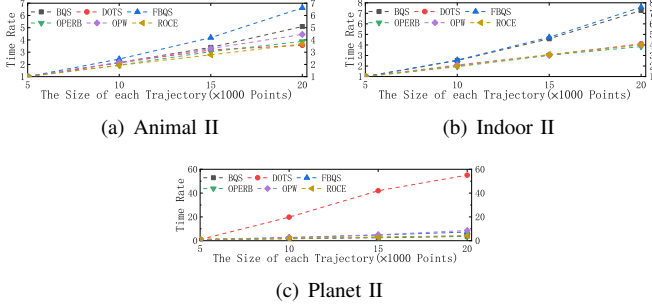


Fig. 13. Efficiency evaluation: varying the size of trajectories

that the tracked object stays at the same place for a long time. On Planet II, the execution time of DOTS is too long when the compression rate is close to 100, so we chose to stop the experiment. Since BQS, FBQS and DOTS are too time-consuming to run on the dataset Planet I, only OPERB, OPW and ROCE were run on Planet I. On Planet I, the execution time of OPERB and ROCE is nearly the same and both becomes shorter with the increase of the compression rate, because fewer trajectory segments are compressed into line segments. Since the time complexity of OPW is $O(N^2)$, the execution time of OPW increases with the increase of the compression rate. ROCE is faster than OPW when the compression rate is more than 100. In summary, ROCE is faster than many other compression algorithms.

To evaluate the impacts of the trajectory size (i.e. the number of points in a trajectory) on the execution time of compression, we chose 20 trajectories, whose sizes are the largest, from Animal, Indoor and Planet respectively, and varied the size of each trajectory from 5000 to 20000, while fixed the compression rate as 50. The results are reported in Figure 13, and the y-coordinates are the rates of the execution time of compressing trajectories to the execution time of compressing trajectories whose trajectory sizes are all 5000. Only algorithms ROCE and OPERB always scale well with the increase of the size of each trajectory on all datasets, and show linear running time. While other algorithms do not, and they need much more time to compress trajectories with more points, especially for DOTS.

2) *Accuracy Loss*: In order to compare the accuracy loss of the compressed trajectories generated by these 6 algorithms,

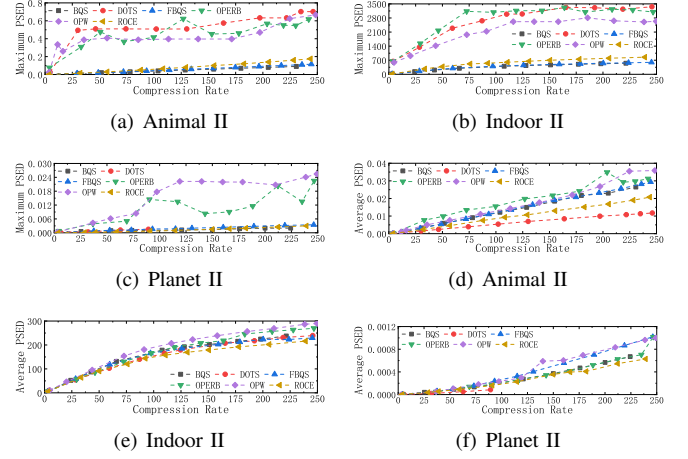


Fig. 14. Evaluation of the maximum PSED and the average PSED: varying the compression rate

we evaluate the maximum PSED and the average PSED of the compressed trajectories w.r.t. varying the compression rate, and the results are shown in Figure 14. For each algorithm, the maximum PSED and the average PSED both increase with the increase of the compression rate. In execution time, ROCE performs similarly with OPERB and OPW, but the maximum PSED of ROCE is always much smaller than those of OPERB and OPW. ROCE, BQS and FBQS always perform similarly in the maximum PSED, but BQS and FBQS need much more execution time than ROCE. On the average PSED, ROCE always performs much better than most other algorithms. So the compressed trajectories generated by ROCE maintain much less accuracy loss than the ones generated by most other algorithms, including other fastest algorithms, i.e. OPW and OPERB. In summary, ROCE makes the best balance among the accuracy loss, the time cost and the compression rate.

C. Performance Evaluation for Range Query Processing Algorithm RQC

In most previous work, each trajectory is seen as a sequence of discrete points. And it's usually regarded that a trajectory is overlapped with the query region R iff at least one point in this trajectory falls in R . In this paper, each compressed trajectory is regarded as a sequence of continuous line segments and a compressed trajectory is overlapped with the query region R iff there is at least one line segment in this compressed trajectory intersecting R . Whether a compressed trajectory is seen as a sequence of discrete points or continuous line segments results in different range query results on compressed trajectories. So in the first following experiment, each compressed trajectory is seen as a sequence of discrete points or continuous line segments and we evaluate the deviation between the range query results on the dataset consisting of raw trajectories and the corresponding compressed dataset. The impacts of the area of each query region, Observation 2 and *ASP-tree* on the execution time of range queries are also studied in the following experiments.

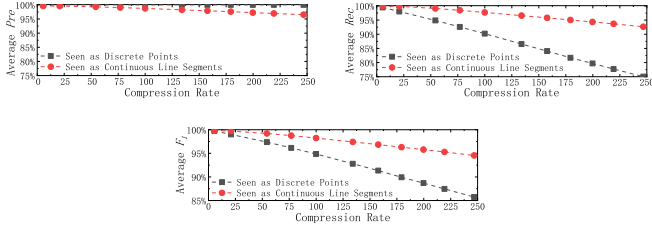


Fig. 15. Evaluation of Pre , Rec and F_1 of range query results on the compressed trajectories: varying the compression rate

Planet I was compressed by ROCE into multiple compressed datasets with different compression rates. The experiments in Section V-C and V-D were all performed on Planet I and its corresponding compressed datasets.

1) *Compressed Trajectories Seen as Discrete Points or Continuous Line Segments*: In order to measure this deviation between the range query results on the raw trajectories and the ones on the corresponding compressed trajectories, we define 3 evaluation metrics. Given a range query, Q_R denotes the range query result set on the raw trajectories, each of which is seen as a sequence of discrete points. And Q_C represents the range query result set on the compressed trajectories. The precision rate Pre and the recall rate Rec of a range query are respectively defined as $Pre = |Q_R \cap Q_C|/|Q_C|$ and $Rec = |Q_R \cap Q_C|/|Q_R|$. For comprehensive comparison, F_1 -Measure is defined as $\frac{F_1}{1} = \frac{1}{2} * (\frac{1}{Pre} + \frac{1}{Rec})$.

We evaluate the average Pre , the average Rec and the average F_1 of 100000 randomly generated range queries on the compressed datasets w.r.t. varying the compression rate, and the results are shown in Figure 15. When each compressed trajectory is seen as a sequence of discrete points, Pre is always 1, since the points in each compressed trajectory must be a subset of the corresponding raw trajectory points. But as the compression rate increases, Rec declines sharply, which means up to 25% trajectories overlapped with the query regions are undiscovered. When each compressed trajectory is seen as a sequence of continuous line segments, though at most 3.5% trajectories not overlapped with the query regions are in the result set, much more trajectories overlapped with the query regions can be found. When each compressed trajectory is regarded as a sequence of continuous line segments, the F_1 is also much higher than the other one. In summary, it's much more accurate to answer range queries on compressed trajectories when each compressed trajectory is regarded as a sequence of continuous line segments.

2) *Impacts of the Areas of Query Regions*: For each range query, the area of the query region has impact on the execution time. 100000 randomly generated range queries were executed on the compressed dataset whose compression rate is 100, and the area of each query region was varied from $5km^2$ to $30km^2$. The results are reported in Figure 16. We can see that the execution time grows approximately linearly with the increase of the area of each query region. And our RQC algorithm is quite efficient and about 30000 range queries can be processed

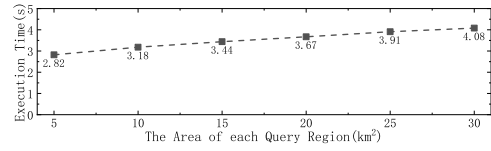


Fig. 16. Efficiency evaluation: varying the area of each query region

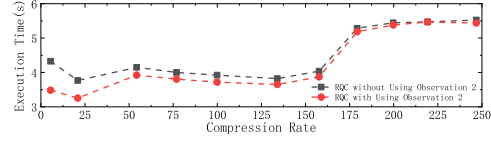


Fig. 17. Efficiency evaluation: Observation 2 when varying the compression rate

in just one second.

3) *Impacts of Observation 2*: To study the impacts of Observation 2, we evaluate the execution time of 10000 randomly generated range queries w.r.t. varying the compression rate, and the results are shown in Figure 17. By using Observation 2, up to 19.5% of the execution time can be saved, and the acceleration gets more obvious when the compression rate gets lower, because for more line segments in compressed trajectories, the positional relationships between them and the query region don't need to be calculated by using Observation 2.

4) *Impacts of ASP-tree*: First, we study how much *ASP-tree* index can accelerate the range query processing. We evaluate the execution time of 10000 randomly generated range queries w.r.t. varying the compression rate, and the results are shown in Figure 18. By using *ASP-tree*, it's obvious that the range query processing can be accelerated greatly, and the execution time can be reduced to less than 1%.

ξ , a threshold value estimated through experiments, controls the average height of *ASP-tree*. The average height of *ASP-tree* is defined as the average height of all leaf nodes, and the height of the root node is 1. We evaluate the average height of *ASP-tree* and the execution time of 100000 randomly generated range queries on the compressed dataset whose compression rate is 100 w.r.t. varying ξ , and the results are shown in Table II. ξ controls the average height of *ASP-tree*, and the average height has impact on the execution time of range queries. The greater the average height of *ASP-tree*, the less execution time needed by these range queries. We also find that the heights of all leaf nodes are almost the same. Especially when $\xi=32000$ or $\xi=64000$, the heights of all leaf nodes are all the same, which shows that *ASP-tree* is not inclined and our region

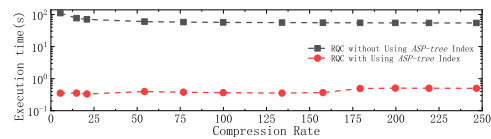


Fig. 18. Efficiency evaluation: *ASP-tree* index when varying the compression rate

TABLE II
EFFICIENCY EVALUATION: VARYING THE THRESHOLD VALUE ξ

ξ	1000	2000	4000	8000	16000	32000	64000
Average Height of <i>ASP-tree</i>	9.64	8.55	7.36	6.11	5.09	5	4
Execution Time (s)	3.48	3.49	5.38	5.33	9.92	10.02	21.89

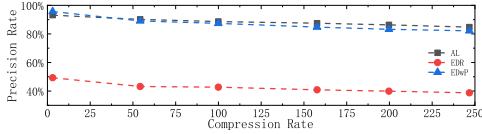


Fig. 19. Evaluation of the average precision rate: varying the compression rate

partitioning strategy dose work.

D. Performance Evaluation for Similarity Query Processing Algorithm *SQC*

In the following experiments, we compare our proposed trajectory similarity metric AL with two other widely used trajectory similarity metrics. The impacts of σ , a threshold value in AL, are also studied. Last, we evaluate the impacts of the *Pre-Punishment* strategy on the execution time of top- k similarity queries.

1) *Trajectory Similarity Metric AL*: We compare AL with two other similarity metrics for measuring the trajectory similarity, namely EDR [11] and EDwP [12]. EDwP is the state-of-the-art metrics for measuring similarity of non-uniform and low sampling rate trajectories. EDR, a trajectory similarity metric based on point, is more robust and accurate than other distance functions [11], [13].

It's challenging to evaluate the accuracy of trajectory similarity because of the lack of ground-truth dataset. To contend with this, we followed the methodology used in previous work [12], [14]. We first randomly chose 20 trajectories from Planet I as top- k similarity query trajectories. Next, we applied each trajectory similarity metrics to get the top- k similarity result of each similarity query from Planet I as its groundtruth. Finally, on the corresponding compressed datasets of Planet I, 20 corresponding compressed trajectories were chosen as top- k similarity query trajectories. And for each query, we got the top- k similarity result from the corresponding compressed dataset using each trajectory similarity metric. Then we compare the result with the corresponding ground-truth. The rationale behind this methodology is that a robust trajectory similarity metric should adapt to compressed trajectories and yield results close to the results on the corresponding raw trajectories.

Figure 19 shows the precision rates (the proportion of true trajectories in top-100 similarity results) of different trajectory similarity metrics when the compression rate of the compressed dataset is varied. The precision of all methods decreases with the increase of the compression rate. EDwP and AL show similar performance, and they both surpass EDR by a fair magnitude. While, the precision of EDwP drops more rapidly when the compression rate increases.

TABLE III
EFFICIENCY EVALUATION: VARYING THE THRESHOLD VALUE σ

σ	0.002	0.004	0.006	0.008	0.01	0.012	0.014	0.016	0.018	0.02
Filtering Rate	99.9%	99.9%	99.9%	99.9%	99.8%	99.8%	99.8%	99.8%	99.8%	99.8%
Execution Time (s)	0.131	0.147	0.162	0.176	0.195	0.212	0.233	0.251	0.269	0.285

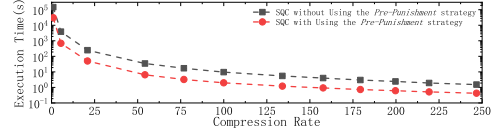


Fig. 20. Efficiency evaluation: the *Pre-Punishment* strategy when varying the compression rate

2) *Impacts of the Threshold Value σ* : σ is a given threshold value and when the minimum Euclidean distance between two compressed trajectories is greater than σ , the similarity between these two compressed trajectories must be 0 in AL. Supposing there are t_q trajectories in the query dataset and t_s trajectories in the similarity candidate set, the filtering rate of the similarity candidate set is defined as $(t_q - t_s)/t_q$. To evaluate the impacts of σ on the filtering rate of the similarity candidate set and the execution time of 10 randomly generated top- k similarity queries on the compressed trajectories, whose compression rate is 100, we varied σ from 0.002 to 0.02 in longitude and latitude, and the results are reported in Table III. With the increase of σ , more trajectories are determined to be similar to the queried one in AL. The filtering rate of the similarity candidate set is at least 99.8%, which means only at most 0.2% trajectories in the queried dataset are left in the similarity candidate set. So by using the similarity candidate set, most of unnecessary calculations of AL can be avoided, and the execution time of top- k similarity queries can be reduced greatly. The execution time increases with the increase of σ , since more trajectories left in the similarity candidate set and more calculations of AL are needed.

3) *Impacts of *Pre-Punishment* strategy*: To study the impacts of the *Pre-Punishment* strategy, we evaluate the execution time of 10 randomly generated similarity queries w.r.t. varying the compression rate, and the results are shown in Figure 20. By using the *Pre-Punishment* strategy, the execution time can be reduced to as low as 17.8%. In Figure 20, there are two execution times measured when the compression rate is 1, i.e., the queried trajectories are raw trajectories. It can be also observed that by querying on the compressing trajectories with a higher compression rate, the execution time of similarity queries can be reduced quite greatly. So it's high efficient to query on the compressed trajectories.

VI. RELATED WORK

Compression algorithms in online mode. Applied in many application scenarios, trajectory compression algorithms in online mode attract people's attention and some algorithms are proposed based on different error criterions. There are mainly 4 frequently-used error criterions, i.e. PED, SED, DAD and LISSED, which measure the degree of the

accuracy loss after a trajectory is compressed. DAD defines the accuracy loss based on the greatest angular difference between two directions. For DAD doesn't take into account the Euclidean distance between each discarded point and its corresponding line segment, a main weakness of DAD is that a discarded point may be too far away from its corresponding line segment and this line segment can't approximately represent such a discarded point well. For each discarded point, SED and LISSED use the time attribute to find its corresponding synchronized point on its corresponding line segment. But the application of SED and LISSED is limited, because the time attribute of each trajectory point isn't always available because of privacy or other reasons. Introduced in Section II-B, PED can be used in much more application scenarios, and there are mainly 4 trajectory compression algorithms in online mode using PED as their error metric, i.e. OPW(BOPW) [6], [7], BQS [1], FBQS [1] and OPERB [5]. OPW is proposed very early and it compresses a trajectory segment as long as possible into a line segment. BQS builds a virtual coordinate system centered at the starting point. In each of 4 quadrants, BQS establishes a rectangular bounding box as well as two bounding lines so that in most cases, a point can be quickly decided for removal or preservation without expensive error calculation. In FBQS, a fast version of BQS, error calculation is no longer needed, and a raw trajectory point is directly reserved if it needs error calculation in BQS. FBQS is a little faster than BQS at the expense of compression rate. Based on a novel distance checking method, OPERB uses a directed line segment to approximate the buffered points. For BQS and FBQS, their accuracy loss is small, but their time cost is extremely high. For OPW and OPERB, relatively less execution time is needed by them, but at the expense of the extremely high accuracy loss.

Trajectory Similarity Metric. Computing the similarity between two trajectories is fundamental functionality in many analysis tasks on trajectories. Based on the distances between matched point pairs of two trajectories, many widely used trajectory similarity metrics have been proposed, such as ED [15], [16], DTW [17], LCSS [18], EDR [11], MA [19] and so on. Among them, EDR is more robust and accurate than other similarity metrics [11], [13]. All of above methods focus on identifying the optimal alignment based on sampled point matching, and thus they are inherently sensitive to variation in the sampling rates and not suitable for compressed trajectories. From another viewpoint of integral, DISSIM [20] defines the spatiotemporal dissimilarity between two trajectories during a definite time interval by integrating their Euclidean distance in time. For DISSIM, two trajectories are determined to be similar iff they must have not only similar movement paths but also similar speeds. But in practical applications, it's not necessary. Designed for measuring the similarity between a pair of raw trajectories under inconsistent and variable sampling rates, EDwP, the state-of-the-art trajectory similarity metric, computes the cheapest set of replacement and insertion operations using linear interpolation to make them identical.

VII. CONCLUSIONS AND FUTURE WORK

In this paper, each compressed trajectory is regarded as a sequence of continuous line segments, but not discrete points. And these continuous line segments approximately describe the movement of the moving object. Based on this, we propose a whole set of solutions to efficient compressing trajectories and querying on compressed trajectories, including a new compression algorithm ROCE, range query processing algorithm RQC and similarity query processing algorithm SQC. An efficient index *ASP-tree* and lots of novel techniques are also presented to accelerate the trajectory compression, range queries and similarity queries obviously.

A couple of issues need to be further studied. In order to further improve the effectiveness of trajectory compression and queries, we are to incorporate methods about trajectory compression methods based on road networks.

ACKNOWLEDGMENT

This work was supported in part by Key Research and Development Projects of the Ministry of Science and Technology under Grant No.2019YFB2101902 and the National Natural Science Foundation of China under Grant No.U19A2059, No.61632010, No.61732003, No.61832003 and No.U1811461.

REFERENCES

- [1] J. Liu, K. Zhao, P. Sommer, S. Shang, B. Kusy, and R. Jurdak, "Bounded quadrant system: Error-bounded trajectory compression on the go," in *2015 IEEE 31st ICDE*, pp. 987–998.
- [2] D. Zhang, M. Ding, D. Yang, Y. Liu, J. Fan, and H. T. Shen, "Trajectory simplification: An experimental study and quality analysis," *Proc. VLDB Endow.*, vol. 11, no. 9, pp. 934–946, 2018.
- [3] B. Ke, J. Shao, Y. Zhang, D. Zhang, and Y. Yang, "An online approach for direction-based trajectory compression with error bound guarantee," in *Asia-Pacific Web Conference*. Springer, 2016, pp. 79–91.
- [4] B. Ke, J. Shao, and D. Zhang, "An efficient online approach for direction-preserving trajectory simplification with interval bounds," in *2017 18th IEEE MDM*, pp. 50–55.
- [5] X. Lin, S. Ma, H. Zhang, T. Wo, and J. Huai, "One-pass error bounded trajectory simplification," *Proceedings of the VLDB Endowment*, vol. 10, no. 7, pp. 841–852, 2017.
- [6] E. Keogh, S. Chu, D. Hart, and M. Pazzani, "An online algorithm for segmenting time series," in *Proceedings 2001 ICDM*, pp. 289–296.
- [7] N. Meratnia and A. Rolf, "Spatiotemporal compression techniques for moving point objects," in *International Conference on Extending Database Technology*. Springer, 2004, pp. 765–782.
- [8] A. Flack, W. Fiedler, J. Blas, I. Pokrovski, B. Mitropolsky, M. Kaatz, K. Aghababayan, A. Khachatryan, I. Fakriadis, E. Makrigianni, L. Jerzak, M. Shamin, C. Shamina, H. Azafzaf, C. Feltrup-Azafzaf, T. Mokoijomela, and M. Wikelski, "Data from: Costs of migratory decisions: a comparison across eight white stork populations," 2015.
- [9] D. Brščić, T. Kanda, T. Ikeda, and T. Miyashita, "Person tracking in large public spaces using 3-d range sensors," *IEEE Transactions on Human-Machine Systems*, vol. 43, no. 6, pp. 522–534, 2013.
- [10] W. Cao and Y. Li, "Dots: An online and near-optimal trajectory simplification algorithm," *Journal of Systems and Software*, vol. 126, pp. 34–44, 2017.
- [11] L. Chen, M. T. Özsu, and V. Oria, "Robust and fast similarity search for moving object trajectories," in *Proceedings of the 2005 ACM SIGMOD International Conference on Management of Data*, pp. 491–502.
- [12] S. Ranu, P. Deepak, A. D. Telang, P. Deshpande, and S. Raghavan, "Indexing and matching trajectories under inconsistent sampling rates," in *2015 ICDE*, pp. 999–1010.
- [13] B. Zhang, Y. Shen, Y. Zhu, and J. Yu, "A gpu-accelerated framework for processing trajectory queries," in *2018 IEEE 34th ICDE*, pp. 1037–1048.

- [14] H. Su, K. Zheng, H. Wang, J. Huang, and X. Zhou, "Calibrating trajectory data for similarity-based analysis," in *Proceedings of the 2013 ACM SIGMOD*, p. 833–844.
- [15] C. Faloutsos, M. Ranganathan, and Y. Manolopoulos, "Fast subsequence matching in time-series databases," in *Proceedings of the 1994 ACM SIGMOD*, p. 419–429.
- [16] B.-K. Yi and C. Faloutsos, "Fast time sequence indexing for arbitrary lp norms," in *Proceedings of the 26th VLDB*, 2000, p. 385–394.
- [17] D. J. Berndt and J. Clifford, "Using dynamic time warping to find patterns in time series," in *KDD workshop*, vol. 10, no. 16, pp. 359–370.
- [18] M. VLACHOS, G. KOLLIOS, and D. GUNOPULOS, "Discovering similar multidimensional trajectories," in *ICDE*, 2002, pp. 673–684.
- [19] S. Sankararaman, P. K. Agarwal, T. Mølhave, J. Pan, and A. P. Boedihardjo, "Model-driven matching and segmentation of trajectories," ser. SIGSPATIAL, 2013, p. 234–243.
- [20] E. Frentzos, K. Gratsias, and Y. Theodoridis, "Index-based most similar trajectory search," in *IEEE ICDE*, 2007.